



An Experiment for Nonlinear an Active Magnetic Bearing System Using Fuzzy Logic Controller

Van-Sum Nguyen¹, Lai Khac Lai^{2(✉)}, and Thanh Hoa Lai²

¹ Department of Mechanics Engineering, Hue Industrial College, Hue, Vietnam

² Thai Nguyen University of Technology, Thai Nguyen, Vietnam
laikhaclai@gmail.com

Abstract. This study presents an intelligent control method for positioning a nonlinear active magnetic bearing (AMB) system by using emergent fuzzy logic controller (FLC). In this work, an AMB system supporting a rotating shaft, without physical contact is presented. By using rotor dynamic model of AMB system and electromagnetic forces of magnetic bearing to design a FLC for an AMB system. The control algorithm was numerically evaluated to construct a multiple-input multiple-output mathematical model of the controlled system. The membership functions and rule design of FLC were based on the mathematical model of an AMB system. A current amplifier and hardware-in-loop (HIL) are used for electromagnetic coil to generate magnetic forces suspended the rotor in magnetic bearing. The results indicated that the system exhibited satisfactory control performance with a low overshooting and produced improved transient and steady-state responses under various operating conditions.

Keywords: Active magnetic bearing · Fuzzy logic controller
Electromagnetic force

1 Introduction

Recently, active magnetic bearings (AMB) have garnered increasing attention because of their practical applications. Magnetic bearings, rather than conventional mechanical bearings, are used in applications that require reduced noise, friction, and vibration [1, 2]. Magnetic bearings are electromechanical devices that use magnetic forces to levitate a rotor without physical contact; magnetic forces are used to suspend the rotor in an air gap. AMB systems depend on reliable control of the air gap between the stator and the rotor. AMB system is highly nonlinear and inherent multiple-input and multiple-output system (MIMOs). Design AMBs controller is not easy and the simulation controller parameters have a little different from the experimental controller parameters. The relationship between the rotor displacement, the current and the electromagnetic force is highly nonlinear. In practice, a precise mathematical model cannot be implemented. Therefore, several nonlinear control techniques have been proposed to address the nonlinear dynamics of the AMB. This study proposes a method for controlling the position of the actuator by using a FLC. The FLCs have recently been successfully

applied to numerous nonlinear systems [3, 4]. Moreover using real time window target (RTWT) rapid control prototyping and hardware-in-loop (HIL) testing, we can quickly change and compare the parameter values. In this work, we use data acquisition (DAQ), current amplifier, and eddy current sensor to setup a HIL testing for AMB system. The proposed design used a FLC to control magnetic bearings and reduce the rotor displacement of an AMB system. The controller also satisfied the real-time response and stability during disturbance requirements of the control system.

2 Structure and Rotor Dynamic of the Active Magnetic Bearings

Many recent studies on magnetic bearings have focused on AMBs. The experimental setup used in this paper is a two axis with symmetric structure, as shown in Fig. 1.

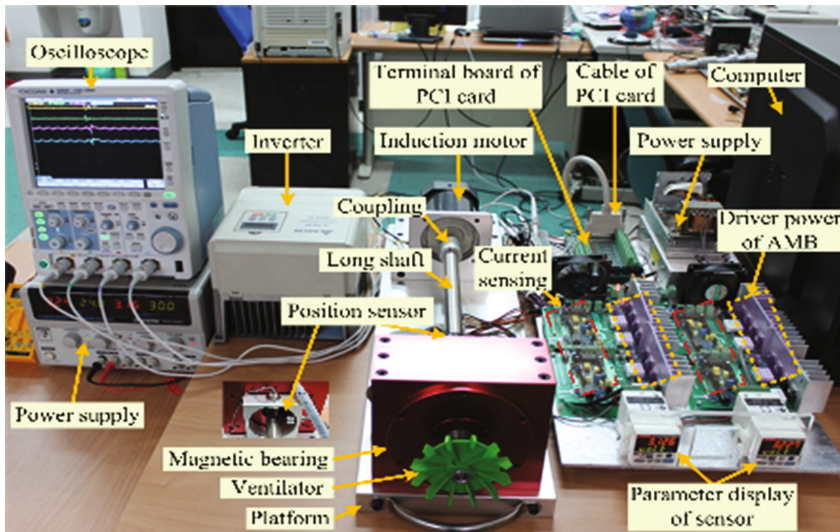


Fig. 1. Photograph of the experimental.

The system is composed of a ventilator, a rotor shaft, a magnetic bearing, a coupling device, a driving motor, and other components. The drive system of the AMB system includes differential driving mode power amplifiers and an analog digital (A/D) converter, as shown in Fig. 2. The variable i_b is the bias current and i_x and i_y are control currents along the x and y axes, respectively. Following Schweitzer and Necip [5, 6], the total nonlinear attractive electromagnetic forces along the x and y axes are given as follows:

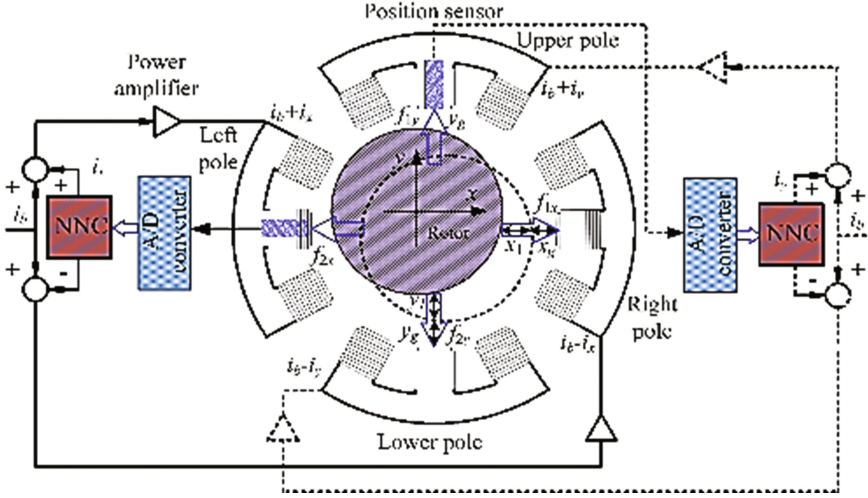


Fig. 2. Drive system of an AMB.

$$f_{1x} - f_{2x} = k \left(\frac{(i_b + i_x)^2}{(x_g - x_1)^2} - \frac{(i_b - i_x)^2}{(x_g + x_1)^2} \right) \quad (1)$$

$$f_{1y} - f_{2y} = k \left(\frac{(i_b + i_y)^2}{(y_g - y_1)^2} - \frac{(i_b - i_y)^2}{(y_g + y_1)^2} \right) \quad (2)$$

where $f_{2x} - f_{1x}$ and $f_{1y} - f_{2y}$ are electromagnetic forces of the magnetic bearings along the x and y axes, respectively; x_1 and y_1 are rotor displacements along the x and y axes; k is the electromagnet constant. In this AMB system, the coil on the x and y axes circulate the same bias current (i_b). Because the nominal air gaps along the x and y axes are also the same ($x_g = y_g$).

The rotor geometry relationships with the center of gravity (CG: x_c, y_c, z_c) in the AMB system is shown in Fig. 3.

where m is the mass of the rotor; g is the gravity constant; $x_c, y_c,$ and z_c are the coordinates of CG; $F_{dx}, F_{dy},$ and F_{dz} are the external disturbance forces of the rotor corresponding to the x, y, and z axes, respectively; $\phi_x, \phi_y,$ and ϕ_z denote the pitch, yaw, and spin angle displacements around the x, y, and z axes of the rotor, respectively; and $l_1, l_2,$ and l_3 are the distances from CG to the flexible coupling, magnetic bearing, and external disturbances, respectively, where $l = l_1 + l_2$. The dynamic equations describing the motion of the rotor bearing system about CG are represented by (3) to (6) [7]

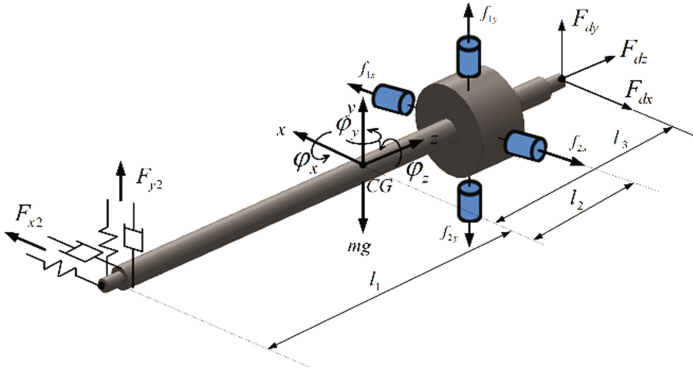


Fig. 3. Geometry relationships of rotor and an AMB system.

$$m\ddot{x}_c = F_{x2} + F_{dx} + f_{1x} - f_{2x} \tag{3}$$

$$J\ddot{\phi}_x + J_z\Omega\dot{\phi}_y = l_1F_{y2} - l_2(f_{1y} - f_{2y}) + l_3F_{dy} \tag{4}$$

$$m\ddot{y}_c = F_{y2} + F_{dy} - mg + f_{1y} - f_{2y} \tag{5}$$

$$J\ddot{\phi}_y - J_z\Omega\dot{\phi}_x = -l_1F_{x2} + l_2(f_{1x} - f_{2x}) + l_3F_{dx}, \tag{6}$$

where J is the transverse moment of inertia of the rigid rotor around its x -axis or its y -axis; J_z is the polar mass moment of inertia of the rotor; $-J_z\Omega\dot{\phi}_x$ and $J_z\Omega\dot{\phi}_y$ are the gyroscopic effects when the rotor rotational speed spinning around the z -axis is Ω ; and F_{x1} and F_{y1} are coupling forces. The dynamic model of the AMB system is indicated as follows,

$$\mathbf{M}_c\ddot{\mathbf{X}}_c + \mathbf{G}_c\dot{\mathbf{X}}_c + \mathbf{K}_{ds}\mathbf{X}_c = \mathbf{K}_{is}\mathbf{u}_c + \mathbf{E}\mathbf{f}_d + \mathbf{D}\mathbf{g} \tag{7}$$

where \mathbf{M}_c is the mass matrix; \mathbf{G}_c is the gyroscopic matrix; \mathbf{K}_{ds} is the displacement stiffness matrix; \mathbf{K}_{is} is the current stiffness matrix; \mathbf{E} is the mass unbalanced external disturbance; \mathbf{f}_d is the external disturbance vector; and \mathbf{D} is gravity vector.

3 Control System Design and Hardware In-Loop for Active Magnetic Bearing System

The FLC controller is designed in RTWT environment for position-control loop. The magnetic bearing has four electromagnetic coils (Left, Right electromagnetic coil for x axis, and Top, Bottom electromagnetic coil for y axis), so we need two controllers for x and y axes of AMB system. The controller diagram of a single degree of freedom (DOF) magnetic bearing is showed in Fig. 4 [8, 9]. The input of FLC in AMB system is the rotor displacement error (e), and the derivative of rotor displacement error (de).

The output of FLC in AMB system is current-control (i_c). The linguistic levels of these inputs and output for x-axis are specified (e_x) as RB: right big, RM: right medium, ZE: zero, LM: left medium, LB: left big. (de_x) as N: negative, NS: negative small, ZE: zero, PS: positive small, P: positive. (i_c_x) as RB: right big, RM: right medium, ZE: zero, LM: left medium, LB: left big. Figures 5, 6 and 7 show the membership functions

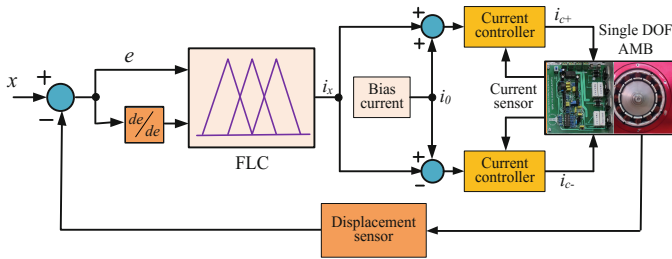


Fig. 4. FLC diagram of the single DOF AMB.

of the inputs and outputs of x axes. Similar for y axis, the linguistic levels of these inputs and output for y-axis are specified (e_y) as TB: top big, TM: top medium, ZE: zero, BM: bottom medium, BB: bottom big. (de_y) as N: negative, NS: negative small, ZE: zero, PS: positive small, P: positive. (i_c_y) as BB: bottom big, BM: bottom medium, ZE: zero, TM: top medium, TB: top big.

Hardware-in-loop (HIL) is rapidly evolving from a control prototyping tool to a system modeling, simulation and testing. The reason of a HIL process becoming more prevalent in all industries is driven by two major factors: time and complexity. HIL process provides an effective platform by adding the complexity of the plant under control to the test platform. The complexity of the plant under control is included in test and development by adding a mathematical representation of all related dynamic systems and a hardware device we want to test. The hardware device is normally an embedded system [10]. Figure 8 displays the HIL of AMB test rig functions using the RTWT with the Matlab/Simulink models.

4 Results and Discussions

The experimental setup of this study is shown in Fig. 1. The laboratory setup included a horizontal shaft magnetic bearing that was symmetrical and controlled by two axes. The system was driven by an induction motor through a flexible coupling to isolate the vibration from the motor. The magnetic bearing included four identical electromagnets that were equally spaced radially around a rotor composed of laminated stainless steel, as indicated in Fig. 9. Each electromagnet included a coil and a laminated core composed of silicon steel.

The output current control for x and y axes are presented in Fig. 10 with bias current is 1 A. Figures 11, 12 and 13 show the rotor displacement and orbit of x and y axes at rotating speeds from 3000 rpm to 13200 rpm. At rotating speeds from 3000 to

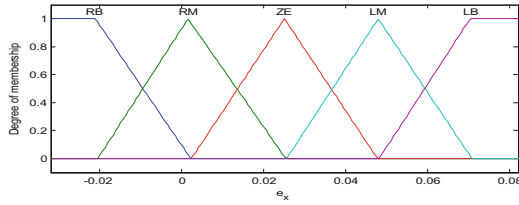


Fig. 5. Membership functions of input e_x .

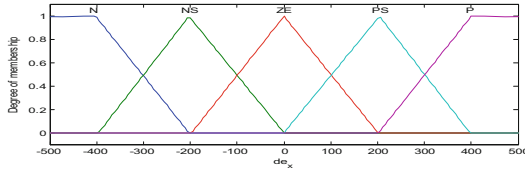


Fig. 6. Membership functions of input de_x .

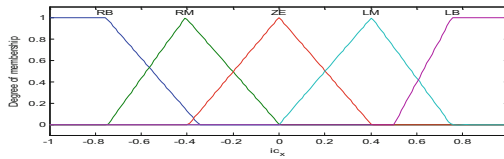


Fig. 7. Membership functions of output ic_x .

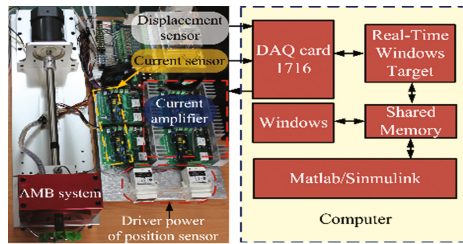


Fig. 8. Hardware-in-loop of AMB test rig functions.

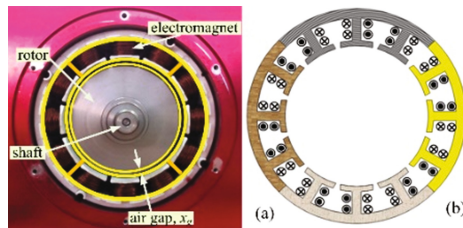


Fig. 9. Photograph of inside view (a) and layout (b) of magnetic bearing.

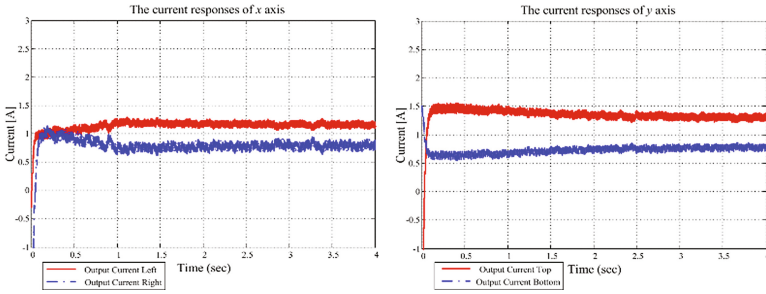


Fig. 10. Current response of x and y axes.

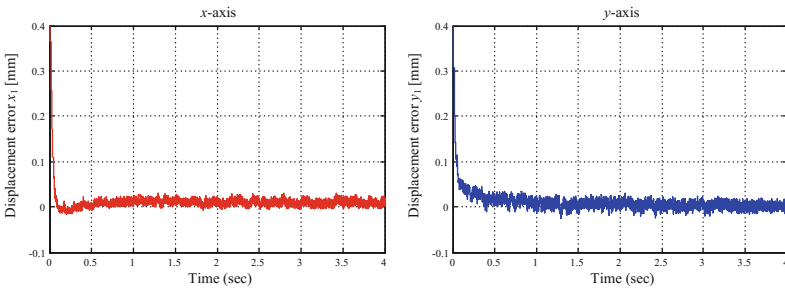


Fig. 11. Rotor displacement x , y axes.

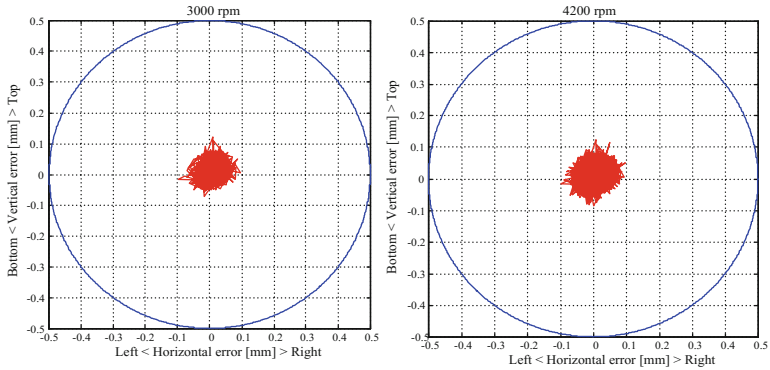


Fig. 12. Orbits of rotor center with 3000 rpm and 4200 rpm.

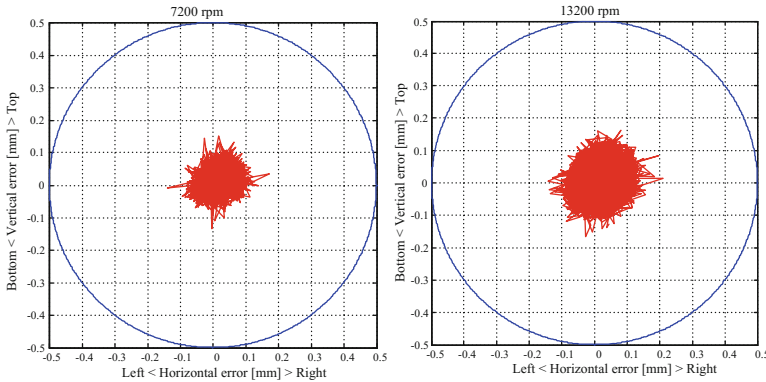


Fig. 13. Orbits of rotor center with 7200 rpm and 13200 rpm.

4200 rpm the rotor displacement is small about 0.07 to 0.12 mm (Fig. 12). When the rotor rotates at high speed (13200 rpm) the rotor displacement is increase about 0.16 to 0.21 mm (Fig. 13) but it is still in the permitted limits of nominal length of air gap ($x_g = 0.5$ mm).

5 Conclusions

This work develops a FLC algorithm that was applied to control for the position loop of AMB system. The results indicated that a FCL allowed the AMB system to achieve more satisfactory performance at various running rotor speeds and unbalanced masses. The results also demonstrated that the AMB system achieved satisfactory dynamic and steady-state responses with rotor rotational speeds between 3000 and 13200 rpm. It shows that the proposed controller schemes allows for a remarkable improvement in reducing vibration in an unbalanced AMB system as well as demonstrate an efficient reduction in the shaft displacement of the rotor. This control method can be used in AMB systems and other nonlinear systems. This controller has been verified by the position-control loop on a prototype AMB system.

References

1. Techn, S.C., Peter, H.C.: Article to the theory and application of magnetic bearings. In: Power Electronics, Electrical Drives, Automation and Motion, vol. 12, pp. 1526–1534 (2012)
2. Chen, S.C., Nguyen, V.S., Le, D.K., Hsu, M.M.: ANFIS controller for an active magnetic bearing system. In: IEEE International Conference on Fuzzy Systems (FUZZ), pp. 1–8 (2013)
3. Chen, S.C., Jyh, L.Y., Nguyen, V.S., Hsu, M.M.: A novel fuzzy neural network controller for maglev system with controlled-PM electromagnets. Lecture Notes in Electrical Engineering, vol. 234, pp. 551–561. Springer (2013)

4. Agarwal, P.K., Chand, S.: Fuzzy logic control of four-pole active magnetic bearing system. In: The 2010 International Conference on Modelling, Identification and Control (ICMIC), pp. 533–538 (2010)
5. Schweitzer, G., Bleuler, H., Traxler, A.: Active magnetic bearings. vdf Hochschulverlag AG. Zürich (1994)
6. Necip, M., Ahu, E.H.: Variable bias current in magnetic bearings for energy optimization. *IEEE Trans. Magn.* **43**, 1052–1060 (2007)
7. Schweitzer, G., Maslen, E.H.: *Magnetic Bearings: Theory: Design and Application to Rotating Machinery*. Springer, Heidelberg (2009)
8. Lin, F.J., Wai, R.J.: Hybrid control using recurrent fuzzy neural network for linear induction motor servo drive. *IEEE Trans. Fuzzy Syst.* **9**, 102–115 (2001)
9. Negnevitsky, M.: *Artificial Intelligence – A Guide to Intelligent Systems*, 2nd edn. (2005)
10. Chiba, A., Fukao, T., Ichikawa, O., Oshima, M., Takemoto, M., Dorrell, D.G.: *Magnetic Bearing and Bearingless Drivers*, pp. 329–342. Elsevier, Jordan Hill, Oxford, UK (2005)